Available online at www.sciencedirect.com

ScienceDirect

IFAC Papers Online CONFERENCE PAPER ARCHIVE

IFAC PapersOnLine 52-20 (2019) 151–156

Networked Model for Cooperative Adaptive Cruise Control

Philip E. Paré * **Ehsan Hashemi** ** **Raphael Stern** ***
Henrik Sandberg * **Karl Henrik Johansson** *

* *Division of Decision and Control Systems at KTH Royal Institute of Technology, Sweden (e-mail: philipar,hsan,kallej@kth.se)*
** *Department of Mechanical and Mechatronics Engineering at University of Waterloo, Canada (e-mail: ehashemi@uwaterloo.ca)*
*** *Department of Informatics at the Technical University of Munich, Germany (e-mail: raphael.stern@tum.de)*

Abstract: This paper proposes a cooperative adaptive cruise control model, adding a communication network structure to an existing model that has been shown to capture real commercial adaptive cruise control vehicle behavior. The proposed model is interesting because it only requires minimal information sharing, facilitating the creation of platoons comprised of vehicles from different manufacturers. We prove the stability of the model and discuss string stability. Algorithms for estimating the velocity of the vehicles locally and for estimating the velocities of all the vehicles in the platoon are presented. We simulate vehicle platoon control with the lead vehicle following an experimentally collected trajectory, showing that adding communication can cause a string unstable platoon to become stable.

Keywords: Semi-autonomous vehicles, Intelligent cruise control, Networks, Traffic control

1. INTRODUCTION

Autonomous vehicles promise to transform mobility and change the way we think about travel. However, before fully autonomous vehicles become commercially available, driver assist features such as adaptive cruise control (ACC) are an important step. ACC is a radar assisted cruise control that monitors the distance to, and relative speed with respect to, the vehicle immediately in front of it, and adjusts the vehicle speed to maintain a safe distance. This feature has been available in luxury vehicles for over a decade, and has recently become a standard feature on many more cars. It has long been speculated that features such as ACC may be able to alter the emergent properties of and even stabilize the traffic flow (Talebpour and Mahmassani, 2016). The relevant notion of stability here is that of string stability, which tells whether a disturbance will dissipate as it propagates from one vehicle to the next in a string of vehicles (Swaroop and Hedrick, 1996).

When analyzing ACC systems, it is desirable to model the vehicle dynamics without having to consider the specifics of the low-level controller. The goal is to capture the second-order (acceleration) dynamics of an ACC vehicle as a function of the vehicle's surroundings. This idea dates back to the early car following models for human driving developed in the 1950s (Gazis et al., 1959), but recently has been applied to model ACC systems using sensor measurements for distance (e.g., radar) as the model inputs. Such car following models generally take the form:

$$\ddot{x}(t) = f(s, \dot{x}, \dot{s}), \tag{1}$$

where the acceleration $\ddot{x}$ is modeled as a function of the space-gap s from the front bumper of the following vehicle to the rear bumper of the lead vehicle, the speed of the following vehicle $\dot{x}$, and the relative speed between the lead vehicle and the following vehicle $\dot{s}$.

One such car following model that has recently been shown to be able to capture the dynamics of commercially available ACC vehicles is the optimal velocity relative velocity (OVRV) model. This model uses a constant time headway [1] policy (similar to the two-second rule often taught to young drivers) along with a gain on the relative velocity with respect to the lead vehicle. The model is string unstable for the headway choices commonly used for commercially-available ACC vehicles (Gunter et al., 2019).

Currently, commercially available ACC vehicles are only able to adjust their driving behavior based on distance measurements made with their on-board sensors. However, with the possibility of vehicle connectivity through dedicated short range communications (DSRC) radios and other technology, connectivity may soon be commonplace on vehicles, opening the possibility of cooperative ACC (CACC) where, in addition to using sensor information about the position of the vehicle in front, a communication network is employed to share relative position, velocity, and acceleration between nearby vehicles.

Vehicle connectivity has long been thought to be one possible way to stabilize autonomous driving systems. It has been shown both theoretically (Levine and Athans, 1966;

[1] Headway is the time gap between the lead vehicle and the following vehicle.

2405-8963
Peer review under responsibility of International Federation of Automatic Control.
10.1016/j.ifacol.2019.12.150

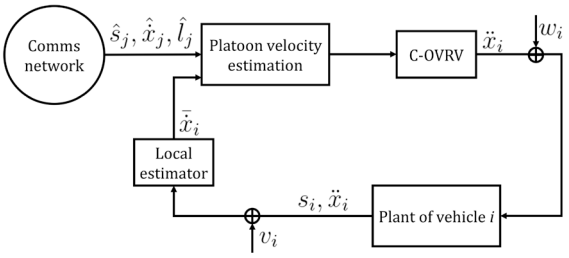

Fig. 1. Overview of proposed modeling framework. Note that the communicated values are for vehicles j in the communication neighborhood $\mathcal{N}_i$.

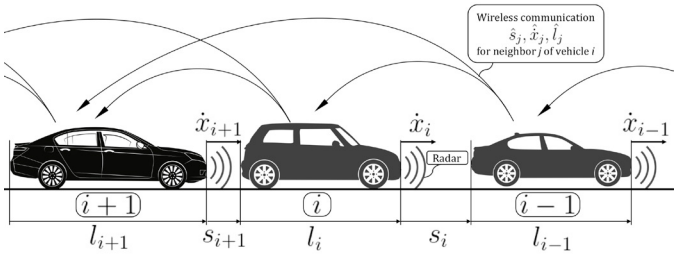

Fig. 2. Platoon configuration showing communication between vehicles.

Swaroop and Hedrick, 1996; Besselink and Johansson, 2017) and experimentally (Ioannou et al., 1993; Shladover, 1995; Milanés et al., 2014) that through connectivity it is possible to form dense vehicle platoons that remain string stable.

Here we propose an extension of the OVRV model (Gunter et al., 2019) that includes network communication, and call it the cooperative-OVRV (C-OVRV) model. It is worth noting that much like the OVRV model, this model is intended to describe vehicle-level car following dynamics, not taking into account the specific low-level controllers that may be present on a vehicle. Therefore vehicles from different manufacturers may form a platoon using this CACC system without sharing those more detailed, possibly proprietary, specifications since each vehicle in the flow only needs to share its spacing s_i, speed $\dot{x}_i$, jam spacing η_i, desired headway τ_i, and vehicle length l_i.

To achieve a networked platoon of vehicles, it is important to be able to accurately estimate the current vehicle state which is being shared via connectivity. Among vehicle states, information about vehicle (longitudinal and lateral) velocity is significant for stability control, road condition estimation, and motion planning (Savitski et al., 2018; Jalali et al., 2016). While such quantities can be measured via GPS, the poor accuracy of available commercial GPSs, particularly in measuring velocity in the lateral direction, and their reliability due to their loss of reception, impede their use in velocity measurements. Therefore, reliable velocity estimation, robust to variations in model parameters and environmental conditions, is vital (Liang et al., 2016; Turri et al., 2017). To this end, a distributed vehicle speed estimation algorithm for arbitrary vehicle networks is presented here. It allows for vehicles with different low-level controllers to share accurate state estimates for platooning. Another advantage is that the local state estimator uses on-board production vehicle sensor data, such as wheel speed and accelerations, to estimate vehicle speed and is robust to road surface friction changes.

The main contributions of this paper are to (1) propose the C-OVRV model; (2) derive the equilibrium of the model, show the system is stable, and discuss string stability; (3) develop algorithms to estimate the true velocity of the vehicles locally and to estimate the states of all the vehicles in the platoon; and (4) simulate the proposed model illustrating the utility of the proposed framework, which is summarized in Figure 1. The paper proceeds as follows. In Section 2 we present the C-OVRV model. We analyze the behavior of the model in Section 3. We present the state estimation algorithms in Section 4. We simulate the system, illustrating that string stability can be achieved via communication, in Section 5. Note, currently Sections 3 and 4 are disconnected however combining everything as in Figure 1 is a future direction.

Notation: For any positive integer n, we use $[n]$ to denote the set $\{1, 2, \ldots, n\}$. We use $\mathbf{0}$ and $\mathbf{1}$ to denote the vectors whose entries all equal zero and one, respectively, I to denote the identity matrix, while the dimensions are to be understood from the context. For any vector $x \in \mathbb{R}^n$, we use $x^\top$ to denote the transpose and $\text{diag}(x)$ or X to denote the $n \times n$ diagonal matrix whose ith diagonal entry equals x_i. We let $\mathrm{e}_i \in \mathbb{R}^n$ be a vector of zeros with the ith entry equal to one and $E_{i,j} \in \mathbb{R}^{n \times n}$ be a matrix of zeros with the i,jth entry equal to one. Given an adjacency matrix A, the Laplacian matrix is defined as $L := \text{diag}(\sum_i [A]_{ij}) - A$, where $[\cdot]_{ij}$ indicates the ijth entry. For a set $\mathcal{A}$ we denote the cardinality of the set by $|\mathcal{A}|$.

2. THE C-OVRV MODEL

OVRV models allow the ACC system of a vehicle to take into account both driving at the optimal velocity and matching the velocity of the vehicle directly in front of it. We adopt the following special case of the OVRV model considered in (Liang and Peng, 1999; Milanés et al., 2014; Gunter et al., 2019), which has been shown to capture the dynamics of commercial ACC systems quite well (Gunter et al., 2019):

$$\ddot{x}_i = f(s_i, \dot{x}_i, \dot{s}_i) = k_1(s_i - \eta_i - \tau_i \dot{x}_i) + k_2 \dot{s}_i \tag{2}$$

where x_i is the position of the front bumper of vehicle i, $s_i := x_{i-1} - x_i - l_{i-1}$ is the space-gap of vehicle i or the distance between the front bumper of vehicle i and the back bumper of the vehicle in front of it (vehicle $i-1$) as seen in Figure 2, the gain parameters k_1 and k_2 correspond to the constant time-headway term and a follow-the-leader term (i.e., match the lead vehicle velocity), respectively, η_i is the jam spacing (the minimum distance two vehicles will attain in steady state), and the parameter τ_i is the desired headway. The lead vehicle, $i = 1$, has the dynamics

$$s_1 = x_c - x_1 \tag{3}$$

where x_c is location of a *phantom vehicle* that represents the trajectory of an imaginary vehicle following a constant speed c that drives in front of the first platoon vehicle. Therefore

$$\dot{s}_1 = c - \dot{x}_1. \tag{4}$$

Now similar to the ideas in (Pirani et al., 2018), we add communication between the vehicles. We expand (2) to the C-OVRV model:

$$\ddot{x}_i = k_1(s_i - \eta_i - \tau_i\dot{x}_i) + k_2\dot{s}_i + w_i + k_3 \sum_{j\in\mathcal{N}_i^+} \left(\hat{\dot{x}}_j - \dot{x}_i\right) + k_4 \sum_{j\in\mathcal{N}_i^+} \left(\hat{x}_j - x_i - \hat{l}_j - \sum_{k=j+1}^{i} (\eta_k + l_k + \tau_k\hat{\dot{x}}_k) + l_i\right), \tag{5}$$

where $\hat{x}_j = \sum_j \left(\hat{s}_j + \hat{l}_j\right)$, and $\hat{s}_j$, $\hat{\dot{x}}_j$, and $\hat{l}_j$ are the spacing, velocity, and length of vehicle j communicated via DSRC, respectively, l_k is the length of vehicle k, $\mathcal{N}_i$ is the set of vehicle i's network neighbors in the communication graph, $\mathcal{N}_i^+$ is the set of vehicles $j \in \mathcal{N}_i$ such that $j < i$, that is, the cars in front of vehicle i that vehicle i can communicate with, and w_i is an unknown disturbance. We assume all the gains are positive.

Remark 1. The communication network can have an arbitrary structure. We only consider one specific static case in this article. Time varying networks and communication delays will be considered in future work. The effect of vehicle yaw rate $\dot{\psi}$ on vehicle longitudinal kinematics is ignored. Thus, the measured longitudinal acceleration can be expressed as the time derivative of longitudinal speed.

Since we want to maintain a stable space gap between the vehicles, we consider the full dynamics in terms of the state variable $(s, \dot{x})$. Therefore we rewrite (5), namely the last term, as a function of the vector of space gaps, s:

$$\ddot{x}_i = k_1(s_i - \eta_i - \tau_i\dot{x}_i) + k_2\dot{s}_i + w_i + k_3 \sum_{j\in\mathcal{N}_i^+} \left(\hat{\dot{x}}_j - \dot{x}_i\right) + k_4 \sum_{j\in\mathcal{N}_i^+} \left(\hat{s}_j + \sum_{k=j+1}^{i} \hat{s}_k - (\eta_k + l_k + \tau_k\hat{\dot{x}}_k)\right). \tag{6}$$

If we assume that the communication is perfect, that is, for all j, $\hat{s}_j = s_j$, $\hat{\dot{x}}_j = \dot{x}_j$, and $\hat{l}_j = l_j$, and if vehicle i can communicate with vehicle j it can also communicate with all vehicles ι, with $j < \iota < i$, then the model can be written in matrix form as

$$\begin{bmatrix}\dot{s}\\ \ddot{x}\end{bmatrix} = \begin{bmatrix}0 & S\\ k_1 I + k_4 D & M\end{bmatrix}\begin{bmatrix}s\\ \dot{x}\end{bmatrix} + \begin{bmatrix}c\,\mathrm{e}_1\\ -k_1\eta - k_4 D(\eta + l) + w\end{bmatrix}, \tag{7}$$

where

$$M = k_2 S - k_3 L - k_1 T - k_4 D T, \tag{8}$$

$$S = \begin{bmatrix}-1 & 0 & 0 & \cdots & 0 & 0\\ 1 & -1 & 0 & \cdots & 0 & 0\\ 0 & 1 & -1 & \cdots & 0 & 0\\ \vdots & & \ddots & \ddots & & \\ \vdots & & & \ddots & \ddots & \\ 0 & 0 & 0 & \cdots & 1 & -1\end{bmatrix}, \tag{9}$$

L is the Laplacian matrix associated with the communication graph determined by the neighbor sets $\mathcal{N}_i^+$, $T = \mathrm{diag}(\tau_i)$,

$$[D]_{ij} = \begin{cases}|\mathcal{N}_i^+| - (i-j) - 1, & \text{if } |\mathcal{N}_i^+| < j \le i\\ 0, & \text{otherwise,}\end{cases} \tag{10}$$

$\eta = [\eta_1, \ldots, \eta_n]^\top$, $l = [l_1, \ldots, l_n]^\top$, and w is the vector of w_i's (the unknown disturbances).

3. ANALYSIS

We now analyze the behavior of the C-OVRV model (7). For the first part of this section, we assume $w_i(t) = 0$ for all $t \ge 0$. Note that S is invertible. Also, with $k_1, k_4 > 0$, since $k_1 I + k_4 D$ is lower triangular with positive diagonal entries, all of its the eigenvalues are greater than zero. Therefore $k_1 I + k_4 D$ is invertible. Thus, the equilibrium of the model is the following:

$$\begin{aligned}\begin{bmatrix}s^*\\ \dot{s}^*\end{bmatrix} &= \begin{bmatrix}0 & S\\ k_1 I + k_4 D & M\end{bmatrix}^{-1}\begin{bmatrix}-c\,\mathrm{e}_1\\ k_1\eta + k_4 D(\eta + l)\end{bmatrix}\\ &= \begin{bmatrix}\hat{M} & (k_1 I + k_4 D)^{-1}\\ S^{-1} & 0\end{bmatrix}\begin{bmatrix}-c\,\mathrm{e}_1\\ k_1\eta + k_4 D(\eta + l)\end{bmatrix}\\ &= \begin{bmatrix}(k_1 I + k_4 D)^{-1}(k_1\eta + k_4 D(\eta + l) - cM\mathbf{1})\\ c\mathbf{1}\end{bmatrix},\end{aligned} \tag{11}$$

where $\hat{M} = -(k_1 I + k_4 D)^{-1} M S^{-1}$.

Given a vector of reference spacings s_r, we have the following equilibrium:

$$\dot{x}^* = M^{-1}(k_1\eta + k_4 D(\eta + l) - (k_1 I + k_4 D)s_r). \tag{12}$$

If we ignore the relative velocity/acceleration parts of the model by setting k_2 and k_3 to zero, the velocities in (12) become

$$\dot{x}^* = (-k_1 T - k_4 D T)^{-1}(k_1\eta + k_4 D(\eta + l) - (k_1 I + k_4 D)s_r).$$

Further simplifying the model by removing the communication network, i.e., setting $k_4 = 0$, gives

$$\dot{x}^* = T^{-1}(s_r - \eta),$$

which is the same equilibrium as the standard heterogeneous OVRV model (Gunter et al., 2019).

Similar to the OVRV model (Monteil et al., 2018), for parameter values as constrained above, the C-OVRV model is always stable.

Proposition 1. The system in (7) converges exponentially to the equilibrium (11).

Proof. Since the system in (7) is affine, it has a unique equilibrium; so if the system is stable it converges to that equilibrium exponentially fast.

Now to show the system is stable, we will show that the system matrix is Hurwitz. Applying a state transformation that reorders the states as $[s_1\ \dot{x}_1\ s_2\ \dot{x}_2\ \cdots\ s_n\ \dot{x}_n]^T$ makes the matrix lower block triangular. The first block is

$$\begin{bmatrix}0 & -1\\ k_1 & -k_1\tau_1 - k_2\end{bmatrix},$$

which has second-order characteristic polynomial equal to $s^2 + (k_1\tau_1 + k_2)s + k_1$. Since all the gains and τ_1 are positive, by the Routh-Hurwitz criterion, these eigenvalues are always strictly negative.

The eigenvalues of the rest of the diagonal blocks follow similarly. Since a block triangular matrix has the same eigenvalues as the union of the eigenvalues of the blocks, the system matrix is Hurwitz. ■

While the stability of the system is essential, a platoon of vehicles requires a higher level of safety, that of string stability, where perturbations do not amplify as they propagate through the platoon (Ploeg et al., 2014). While

the definition in (Ploeg et al., 2014) is applicable for ACC systems since the dynamics of vehicle i are only a function of vehicle $i-1$, this is not the case for the C-OVRV model. Therefore, similar to the ideas in (Middleton and Braslavsky, 2010; Besselink and Knorn, 2018) we propose the following definition that will be discussed via simulation in Section 5.

Definition 1. A platoon of n vehicles with communication is considered to be *string stable* if there exists a uniform bound γ such that, for all n,

$$\left\| [0\ I] \left(sI - \begin{bmatrix} 0 & S \\ k_1 I + k_4 D & M \end{bmatrix} \right)^{-1} \begin{bmatrix} 0 \\ I \end{bmatrix} \right\|_{\mathcal{H}_\infty} < \gamma.$$

4. STATE ESTIMATION IN A VEHICULAR NETWORK

The previous sections assume perfect measurements and communication. However, we know that sensors are not completely accurate all of the time. To enable networked platoon control of vehicles without knowledge of the specific low-level controller of each vehicle, it is important to have accurate estimates of each vehicles' states. Therefore, in this section, we first propose an estimation algorithm that estimates the true longitudinal velocities using a parameter-varying observer. Then we proceed to present a vehicle-local algorithm that estimates the velocities of the whole platoon, not only the network neighbors, employing the velocity estimates via the communication network.

4.1 Local state estimation in the physical layer

Vehicle accelerations $\hat{\dot{x}}_j$ measured by local inertial measurement units (IMUs) can be directly communicated via DSRC, but longitudinal speeds $\hat{x}_j$, which are significant contributors not only in the developed C-OVRV model, but in local low-level stability and traction control of each individual vehicle, need to be estimated. To this end, and to model the longitudinal dynamics of each individual vehicle, the vehicle kinematics and LuGre tire model Canudas-de Wit et al. (2003) are combined to obtain a kinematic-tire model based system with states $\xi_i = [z_{t_i} \quad v_{r_i}]^\top$, where z_{t_i} is an internal LuGre tire state and v_{r_i} is relative longitudinal speed caused by slip at each tire of vehicle i, as shown in Fig. 3. The input term is $\bar{u}_i = R_i\dot{\omega}_i - a_{x_{t_i}}$, where $\dot{\omega}_i$ is wheel acceleration and $a_{x_{t_i}}$ is corner acceleration, which is measured by a local IMU and mapped to four vehicle corners (tires). The dynamics evolve as

$$\dot{\xi}_i = A_{v_i}(\omega_i)\xi_i + B_v\bar{u}_i + \bar{w}_i$$

with

$$A_{v_i}(\omega_i) = \begin{bmatrix} -\zeta_i R_i\omega_i & 1 \\ 0 & 0 \end{bmatrix},$$

where ζ_i is a tire parameter, $\omega_i \in \mathbb{R}^+$ is the wheel speed (and is treated as a bounded time-varying parameter), R_i is the tire radius, $B_v = [0 \quad 1]^\top$, and $\bar{w}_i$ captures the model uncertainties (due to tire forces and noises in acceleration and wheel speed measurements). Then, by implementing measured vehicle accelerations and wheel speeds at each vehicle tire, a parameter-varying observer is designed in Hashemi et al. (2017) as

$$\dot{\hat{\xi}}_i = A_{v_i}(\omega_i)\hat{\xi}_i + B_v\bar{u}_i + \mathcal{L}(f_i - \hat{f}_i), \tag{13}$$

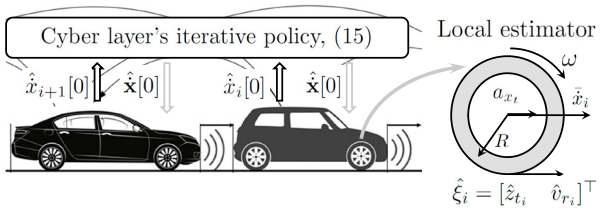

Fig. 3. Local observers and distributed speed estimation in the cyber layer

to estimate longitudinal speed for each vehicle in the network. $\mathcal{L} \in \mathbb{R}^2$ includes local observer gains $\mathcal{L}_1, \mathcal{L}_2$ and the estimated output is related to the states as $\hat{f}_i = C_{v_i}(\omega_i)\hat{\xi}_i + C_{B_i}B_v\bar{u}_i$ with $C_{B_i} = [p_{2_i} \quad 0]]$ and $C_{v_i}(\omega_i) = [p_{1_i} - p_{2_i}\zeta_i R_i\omega_i \quad p_{2_i} + p_{3_i}]$, in which $p_{1_i}, p_{2_i}, p_{3_i}$ are tire parameters. The error dynamics $\tilde{\dot{\xi}}_i = \dot{\xi}_i - \dot{\hat{\xi}}_i$ yields

$$\tilde{\dot{\xi}}_i(t) = \tilde{A}_{v_i}(\omega_i)\tilde{\xi}_i + \tilde{B}_{v_i}\bar{w}_i, \tag{14}$$

where $\tilde{A}_{v_i}(\omega_i) = A_{v_i}(\omega_i) - \mathcal{L}C_{v_i}$ and

$$\tilde{B}_{v_i} = \begin{bmatrix} 1 - \mathcal{L}_1 p_{2_i} & 0 \\ -\mathcal{L}_2 p_{2_i} & 1 \end{bmatrix}.$$

Proposition 2. The local speed estimator error dynamics in (14) are stable for bounded feasible wheel speed $\omega_i \in [\omega_i^l, \omega_i^u]$.

The stability of the local speed estimator (13) is proved and its performance is investigated in (Hashemi et al., 2017) based on affine quadratic stability and affine quadratic $\mathcal{H}_\infty$ performance.

Remark 2. The locally estimated speed of each vehicle is calculated as $\bar{x}_i = (R_i\omega_i - \hat{v}_{r_i})\cos\delta_i$, where δ_i is the steering angle of wheel of vehicle i and $\hat{v}_{r_i}$ is the estimate from the state observer (13).

For the discrete-time distributed scheme, from here on, the estimated speed in the cyber layer is denoted by $\hat{x}_i[\kappa]$. All local estimates $\bar{x}_i$ are sent to the cyber layer as initial conditions $\hat{x}_i[0]$ (for the iterative policy (15)) and, at each time step, are treated as components of vehicle i's measurement vector $y_i[\kappa]$ that it has access to (its own speed and the speed values of its neighbors).

4.2 Distributed speed estimation

This subsection focuses on the performance of a distributed speed estimation scheme in terms of graph-theoretic properties for cooperative adaptive cruise control. Due to the nature of distributed calculation via communication, in this subsection, the updating rules and observability analysis are provided in discrete-time. The objective is for vehicle i, that is not in the communication range of vehicle j, to estimate the speed of vehicle j, denoted by $\hat{x}_j[0]$. Vehicle i obtains its own speed, $\bar{x}_i$, using the local state estimator in (13) (as explained in Remark 2), and the speed of other vehicles within its communication range, $\mathcal{N}_i$, employing information from both front and rear neighbors, at each time step $t_\kappa = \kappa T_s$, where T_s is the sampling time. More formally, implementing the following updating rule, similar to (Pirani et al., 2018), vehicle i executes a distributed consensus policy that incorporates the estimated velocities of its network neighbors with some positive arbitrary gains ϕ_i^i, ϕ_j^i:

$$\hat{\hat{x}}_i[\kappa+1] = \phi_i^i \hat{\hat{x}}_i[\kappa] + \sum_{j\in\mathcal{N}_i} \phi_j^i \hat{\hat{x}}_j[\kappa], \tag{15}$$

where $\hat{\hat{x}}_j[\kappa]$ represents an estimate of the longitudinal speed of vehicle j at time κ that incorporates the shared information via the communication network. The aim of such information dissemination is for each vehicle to calculate the initial conditions of all other vehicles after running the linear dynamics (15), which occurs in the cyber layer, after several time steps as shown in Figure 3. The vector form of the iteration policy (15) yields $\hat{\hat{\mathbf{x}}}[\kappa+1] = \Phi\hat{\hat{\mathbf{x}}}[\kappa]$, where $\hat{\hat{\mathbf{x}}} = [\hat{\hat{x}}_1, \ldots, \hat{\hat{x}}_2]^\top$. The components of matrix $\Phi \in \mathbb{R}^{n\times n}$ are positive arbitrary weights ϕ_j^i, but $\Phi_{ij} = 0$ if $j \notin \mathcal{N}_i \cup \{i\}$. Vehicle i receives the speed of its neighbors and has access to its own speed, thus, the measurement vector for vehicle i is $y_i[\kappa] = C_i\hat{\hat{\mathbf{x}}}[\kappa]$, at each time step, where C_i is a $(|\mathcal{N}_i|+1)\times n$ matrix with each row equal to e_j for $j \in \mathcal{N}_i \cup \{i\}$. The updating rule (15) enables each vehicle to estimate the speed of other vehicles, $\hat{\hat{\mathbf{x}}}[0]$ after some time steps, and updates the velocity estimates $\hat{\hat{x}}_i[\kappa]$, in the cyber layer.

Problem 1. Given the model in (15) and local speed estimation from (13), find the necessary and sufficient conditions that guarantee vehicle i can correctly estimate the longitudinal velocities of all the vehicles in the platoon.

The set of available measurements for vehicle i during the first $q+1$ time steps is

$$y_i[0:q-1] = \mathcal{O}_{i,q}\hat{\hat{\mathbf{x}}}[0], \tag{16}$$

where $\mathcal{O}_{i,q} = [C_i; \quad C_i\Phi; \quad C_i\Phi^2\mathcal{A}_d \ldots C_i\Phi^q\mathcal{A}_d^{q-1}]^\top$ is the observability matrix. The discrete-time state transition matrix $\mathcal{A}_d = e^{\mathcal{A}T_s}$ from the system (7) with

$$\mathcal{A} = \begin{bmatrix} 0 & S \\ k_1 I + k_4 D & M \end{bmatrix}$$

is taken into account to include the interconnection between the local observers in the physical layer and the distributed calculation algorithm in the cyber layer. Having full column rank of the observability matrix $\mathcal{O}_{i,q}$ (observability condition) allows vehicle i to correctly estimate the initial speed of the rest of the vehicles. Based on *Theorem 2* in Sundaram and Hadjicostis (2008), we can conclude that for almost any choice of gain matrix Φ, such that the observability matrix is guaranteed to be full column rank, vehicle i can estimate $\hat{\hat{x}}_j[0]$ after $q+1$ time steps for a bounded value of q that depends on $|\mathcal{N}_i|$ and $\max_{j\in[n]}\{|i-j|\}$.

5. NUMERICAL EXPERIMENTS

In this section, numerical experiments are conducted with the model proposed in (5) using k-nearest neighbor graphs ($|\mathcal{N}_i^+| = k$) to demonstrate how the model can be used to simulate platoon dynamics, and explore the influence of the communication neighborhood size on string stability. The parameter values for k_1, k_2, τ, and l in the simulations were those found in (Gunter et al., 2019, under review) from real commercial vehicles, $k_3 = k_4 = 0.3$ (chosen arbitrarily), and the lead vehicle follows an experimentally collected vehicle trajectory presented in (Gunter et al., 2019, under review).

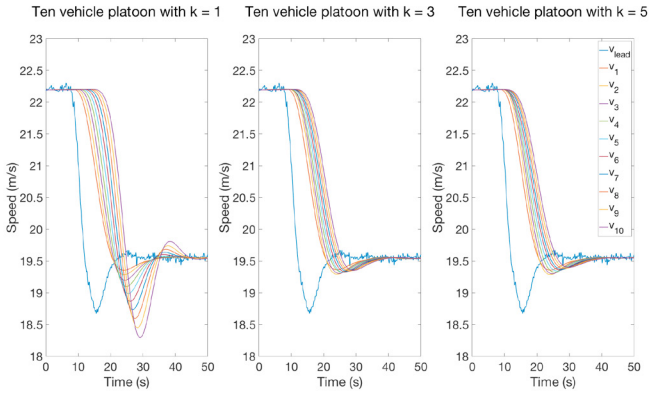

Fig. 4. Platoon simulation of three homogeneous platoons with $n = 10$ CACC vehicles that all follow the dynamics in (2) with $k_1 = 0.08$, $k_2 = 0.44$, $k_3 = 0.30$, $k_4 = 0.30$, $\tau = 0.52$, $\eta = 8.34$, and $l = 4.89$. The size of the communication neighborhood k is varied to show the influence of the radius communication network on the degree of overshoot in braking. The speed overshoot of successive vehicles in the platoon indicates string instability, since the initial perturbation is amplified through the vehicle platoon.

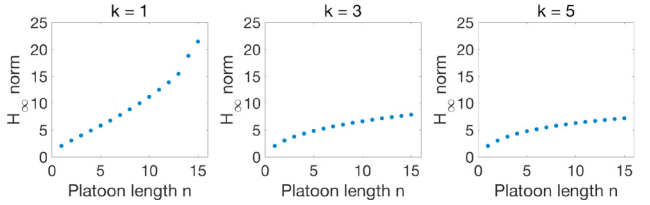

Fig. 5. Using Definition 1 we plot the H_∞ norm of the systems in Figure 4 against the size of the platoon n.

In Figure 4 the velocities of a homogeneous platoon of $n = 10$ vehicles are shown. In the dataset, the lead vehicle starts at a constant speed of roughly 22 m/s (50 mph) and, after roughly 10 seconds, the lead vehicle decelerates to 19.7 m/s (44 mph). The communication radius k is increased from $k = 1$ neighbor in the first plot to $k = 5$ neighbors in the last plot. The result is that when the communication radius is increased, the same vehicle parameter values go from being string unstable to being string stable.

The string instability is illustrated by the amplification of the perturbation as it propagates through the platoon. As the platoon gets larger this amplification would cause vehicles to go below the minimum velocity and switch off the CACC system, therefore splitting the platoon. Note that $k = 1$ makes the C-OVRV model equivalent to the OVRV model, i.e. no communication. Therefore, these simulations show that under realistic parameter values, i.e. on real vehicles, adding communication to an string unstable platoon can make it string stable. Note that the first CACC vehicle follows the lead vehicle with a greater headway than the remaining CACC vehicles. This is because there is no connectivity between the experimental lead vehicle and the platoon of CACC following vehicles.

To explore the string stability of the system in more detail using Definition 1, we calculated the $\mathcal{H}_\infty$ norm of the systems in Figure 4 varying the size of the platoon n. The results are presented in Figure 5. Note how for $k = 1$

the norm appears to increase without bound with n while for $k = 3$ and $k = 5$, the $\mathcal{H}_\infty$ norm appears to approach some bound γ, consistent with the simulations in Figure 4, where the simulation with $k = 1$ is string unstable, while the simulations for $k = 3$ and $k = 5$ are stable. For future work, we will provide a rigorous proof of this phenomenon, characterizing γ in terms of the model parameters.

6. CONCLUSION

In this paper we proposed the C-OVRV model which adds a communication network to the OVRV model for ACC systems to make it a CACC system. We performed some preliminary analysis on the model, proving stability. We proposed a distributed estimation algorithm that allows vehicles to locally estimate the velocities of all the vehicles in the platoon. We simulated the model using real data as our phantom lead vehicle, illustrating how the model can exhibit both string stable and unstable behavior, and how communication may remove the instability. We also explored the string stability of the system via simulation.

For future work we would like to perform further analysis on the model, providing a necessary and sufficient condition for string stability, characterizing γ from Definition 1 in terms of the model parameters. We would also like to integrate the distributed estimation algorithm into the C-OVRV model, allowing vehicle i to include the estimated velocities of the rest of the platoon in its velocity update, completing the loop in Figure 1. Further, we would like to implement this system on a real platoon and experimentally verify the theoretical and simulation results.

REFERENCES

Besselink, B. and Johansson, K.H. (2017). String stability and a delay-based spacing policy for vehicle platoons subject to disturbances. *IEEE Transactions on Automatic Control*.

Besselink, B. and Knorn, S. (2018). Scalable input-to-state stability for performance analysis of large-scale networks. *IEEE Control Systems Letters*.

Canudas-de Wit, C., Petersen, M.L., and Shiriaev, A. (2003). A new nonlinear observer for tire/road distributed contact friction. In *Proceedings of the 42nd IEEE Conference on Decision and Control*, 2246–2251.

Gazis, D.C., Herman, R., and Potts, R.B. (1959). Car-following theory of steady-state traffic flow. *Operations Research*, 7(4), 499–505.

Gunter, G., Gloudemans, D., Stern, R.E., McQuade, S., Bhadani, R., Bunting, M., Delle Monache, M.L., Lysecky, R., Seibold, B., Sprinkle, J., Piccoli, B., and Work, D.B. (2019, under review). Are commercially implemented adaptive cruise control systems string stable? *Submitted to IEEE Transactions on Control Systems Technology*.

Gunter, G., Janssen, C., Barbour, W., Stern, R.E., and Work, D.B. (2019). Model based string stability of adaptive cruise control systems using field data. *arXiv*. ArXiv:1902.04983v1 [cs.SY].

Hashemi, E., Pirani, M., Khajepour, A., Kasaiezadeh, A., Chen, S.K., and Litkouhi, B. (2017). Corner-based estimation of tire forces and vehicle velocities robust to road conditions. *Control Engineering Practice*.

Ioannou, P., Xu, Z., Eckert, S., Clemons, D., and Sieja, T. (1993). Intelligent cruise control: theory and experiment. In *Proceedings of the 32nd IEEE Conference on Decision and Control*, 1885–1890.

Jalali, M., Khajepour, A., Chen, S.k., and Litkouhi, B. (2016). Integrated stability and traction control for electric vehicles using model predictive control. *Control Engineering Practice*, 54, 256–266.

Levine, W. and Athans, M. (1966). On the optimal error regulation of a string of moving vehicles. *IEEE Transactions on Automatic Control*, 11(3), 355–361.

Liang, C.Y. and Peng, H. (1999). Optimal adaptive cruise control with guaranteed string stability. *Vehicle System Dynamics*, 32(4-5), 313–330.

Liang, K.Y., Mårtensson, J., and Johansson, K.H. (2016). Heavy-duty vehicle platoon formation for fuel efficiency. *IEEE Transactions on Intelligent Transportation Systems*, 17(4), 1051–1061.

Middleton, R.H. and Braslavsky, J.H. (2010). String instability in classes of linear time invariant formation control with limited communication range. *IEEE Transactions on Automatic Control*, 55(7), 1519–1530.

Milanés, V., Shladover, S.E., Spring, J., Nowakowski, C., Kawazoe, H., and Nakamura, M. (2014). Cooperative adaptive cruise control in real traffic situations. *IEEE Transactions on Intelligent Transportation Systems*, 15(1), 296–305.

Monteil, J., Bouroche, M., and Leith, D.J. (2018). L_2 and L_∞ stability analysis of heterogeneous traffic with application to parameter optimization for the control of automated vehicles. *IEEE Transactions on Control Systems Technology*, (99), 1–16.

Pirani, M., Hashemi, E., Fidan, B., Simpson-Porco, J.W., Sandberg, H., and Johansson, K.H. (2018). Resilient estimation and control on k-nearest neighbor platoons: A network-theoretic approach. 51(23), 22 – 27. 7th IFAC Workshop, NECSYS 2018.

Ploeg, J., Van De Wouw, N., and Nijmeijer, H. (2014). Lp string stability of cascaded systems: Application to vehicle platooning. *IEEE Transactions on Control Systems Technology*, 22(2), 786–793.

Savitski, D., Schleinin, D., Ivanov, V., and Augsburg, K. (2018). Robust continuous wheel slip control with reference adaptation: Application to brake system with decoupled architecture. *IEEE Transactions on Industrial Informatics, DOI: 10.1109/TII.2018.2817588*.

Shladover, S.E. (1995). Review of the state of development of advanced vehicle control systems (AVCS). *Vehicle System Dynamics*, 24(6-7), 551–595.

Sundaram, S. and Hadjicostis, C.N. (2008). Distributed function calculation and consensus using linear iterative strategies. *IEEE Journal on Selected Areas in Communications*, 26(4), 650–660.

Swaroop, D. and Hedrick, J. (1996). String stability of interconnected systems. *IEEE Transactions on Automatic Control*, 41(3), 349–357.

Talebpour, A. and Mahmassani, H.S. (2016). Influence of connected and autonomous vehicles on traffic flow stability and throughput. *Transportation Research Part C: Emerging Technologies*, 71, 143–163.

Turri, V., Besselink, B., and Johansson, K.H. (2017). Cooperative look-ahead control for fuel-efficient and safe heavy-duty vehicle platooning. *IEEE Transactions on Control Systems Technology*, 25(1), 12–28.